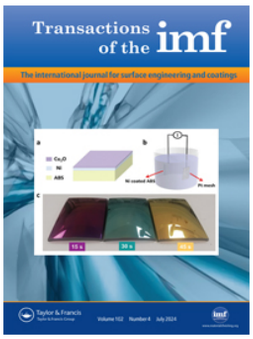

Taylor & Francis
Taylor & Francis Group

Transactions of the IMF
The International Journal of Surface Engineering and Coatings

ISSN: 0020-2967 (Print) 1745-9192 (Online) Journal homepage: www.tandfonline.com/journals/ytim20

Electrochemical deposition of coloured Ni/Cu_2O bilayer films on large area plastic substrates for decorative applications

Suleyman Can, Alime Colak, Huseyin Balci & Cihan Kuru

To cite this article: Suleyman Can, Alime Colak, Huseyin Balci & Cihan Kuru (2024) Electrochemical deposition of coloured Ni/Cu_2O bilayer films on large area plastic substrates for decorative applications, Transactions of the IMF, 102:4, 183-189, DOI: 10.1080/00202967.2024.2365056

To link to this article: https://doi.org/10.1080/00202967.2024.2365056

TRANSACTIONS OF THE IMF
2024, VOL. 102, NO. 4, 183–189
https://doi.org/10.1080/00202967.2024.2365056

Electrochemical deposition of coloured Ni/Cu_2O bilayer films on large area plastic substrates for decorative applications

Suleyman Can [a], Alime Colak[b], Huseyin Balci[b] and Cihan Kuru [a]

[a]Department of Metallurgical and Materials Engineering, Bilecik Seyh Edebali University, Bilecik, Turkey; [b]Durden Plastic Products and Adhesive Films Inc., Bilecik, Turkey

ABSTRACT

In this study, coloured Ni/Cu_2O bilayer films were electrochemically deposited on large area automobile plastic parts (7 × 13 cm) for decorative applications. Such coatings may become an alternative to ubiquitously used Cr coatings for plastics. Purple, dark cyan and gold colours with good homogeneity and high brightness could be produced by tuning the deposition time of the Cu_2O layer. Colouration of the bilayer film can be ascribed to interference of light through the metal/dielectric layer, where the thickness of the dielectric layer controls the wavelength of the reflected light. Cu_2O film has a compact structure and low roughness, which is essential to obtain uniform colours. Moreover, the Ni/Cu_2O bilayer exhibits good adhesion behaviour, environmental stability and enhanced corrosion resistance. This process is industrially viable and enables the large scale production of such decorative coatings.

ARTICLE HISTORY
Received 7 May 2024
Accepted 3 June 2024

KEYWORDS
Decorative coatings; electrochemical deposition; plastics; structural colours; Cu_2O

1. Introduction

Inspired by nature, structural colours have drawn great attention owing to high degree of tunability, aesthetic look and authentic feel. Unlike dye-based colours, structural colours consist of inorganic materials which are more resistant to UV light and mechanical wear. Such colours can be created by the interaction of light with surface structures. Photonic crystals, plasmonic nanostructures and diffraction gratings have been demonstrated to generate structural colours.[1–4]. Light propagation can be controlled by the shape, size and the periodicity of the structures, leading to a colouring effect.[5] Although these structures are highly effective to produce a wide gamut of colours, the complex fabrication procedure and high manufacturing cost hinder their practical applications.

Alternately, Fabry–Perot (F-P) cavities can be utilised to produce structural colours. F-P cavities have a multilayer structure consisting of a dielectric layer sandwiched by two metal layers.[6] F-P cavities filter out the light of a certain wavelength depending on the thickness of the dielectric layer.[6] Therefore, the colour of the reflected light can be tuned by modulating the thickness of the dielectric layer. The hue of the colour can also be adjusted by varying the thickness of the top metal layer.[7] Various materials have been tested for F-P cavities, where metal and dielectric layers are usually deposited using vacuum deposition techniques.[8–11]

The use of industrially viable processes such as electrochemical deposition is highly appealing for mass production of structural coloured coatings. Electrochemical deposition has been widely used in the automotive industry for the deposition of Cu/Ni/Cr multilayer coatings to add an aesthetic look to plastic parts. Here, the authors fabricated coloured Ni/Cu_2O coatings on large area ABS (Acrylonitrile Butadiene Styrene) plastic parts by electrochemical deposition as an alternative to Cr for the automotive industry. Such metal/dielectric bilayer coatings offer a more simplified approach to obtain a colouring effect based on interference phenomena. The metal/dielectric bilayer approach was adopted rather than F-P cavities because it is extremely challenging to deposit ultrathin top metal layers on a dielectric layer by electrochemical deposition. Moreover, Cu_2O was chosen as the dielectric material owing to the feasibility of the electrochemical deposition of compact Cu_2O films with controlled thickness.[12] Although various coloured bilayer coatings including Cu/CuO,[13] Ti/SiN,[14] Au/CuO[15] and Ag/Ag_2O[16] have been previously demonstrated, electrochemical deposition of such coatings on plastic substrates has not been achieved. In the current study, purple, dark cyan and gold colours could be achieved, with high brightness and homogeneity by simply tuning the deposition time of the Cu_2O film. The morphology and the thickness of the Ni/Cu_2O bilayer film were evaluated by scanning electron microscopy (SEM) and atomic force microscopy (AFM) measurements. The chemical composition and crystal structure were determined by energy-dispersive X-ray spectroscopy (EDX) and X-ray diffraction (XRD) measurements. The optical properties were investigated by reflectance measurements and adhesion of the film was assessed by cross-cut tests.

2. Experimental methods

2.1. Ni electroplating on ABS

The ABS surface was first cleaned in an alkaline bath and subsequently etched in a mixture of chromic acid (H_2CrO_4, Şişecam, 99%) and sulphuric acid (H_2SO_4, Carlo Erba, 98%) at 70°C for 15 min to increase the wettability and surface

CONTACT Cihan Kuru cihan.kuru@bilecik.edu.tr Department of Metallurgical and Materials Engineering, Bilecik Seyh Edebali University, Bilecik 11230, Turkey

Supplemental data for this article can be accessed online at https://doi.org/10.1080/00202967.2024.2365056.

area. After the etching process, the ABS was neutralised in a sodium bisulphite ($NaHSO_3$, UCN Chemical, 99%) solution, which converted Cr^{+6} to Cr^{+3}. To activate the ABS surface for the electroless Ni deposition, ABS was first immersed in stannous chloride ($SnCl_2$, Silken) and hydrochloric acid (HCl) mixture and then in palladium chloride ($PdCl_2$, Silken) and HCl mixture at 40°C. Following this, excess Sn^{+2} ions were removed in sodium hypophosphite (NaH_2PO_2, Silken) at 40°C for a few minutes. The ABS surface was metallised by electroless Ni deposition, which was conducted in a bath containing nickel chloride ($NiCl_2$, ErametSelnic, 98%) (20 g L^{-1}), NaH_2PO_2 (20 g L^{-1}), sodium citrate ($Na_3C_6H_5O_7$, ZAG, 99%) (45 g L^{-1}) and ammonium chloride (NaH_4Cl, ZAG, 99%) (30 g L^{-1}) at 80°C for 5 min. Ni electroplating was carried out under a current density of 5 A dm^{-2} for 15 min at 55°C in a plating bath of nickel sulphate hexahydrate ($NiSO_4.6H_2O$, Nickelhütte Aue) (275 g L^{-1}), $NiCl_2$ (55 g L^{-1}), boric acid (H_3BO_3, EtiMaden, 99%) (45 g L^{-1}), brightener Spectra 77 (Growel) (0.3 mL L^{-1}) and Ni additive 22 (Growel) (3 mL L^{-1}). The overall thickness of the Ni film was 25–30 µm, measured using a coulometric thickness gauge (Fischer Couloscope Cms2 STEP). The whole process was conducted in an industrial fully automated system.

2.2. Electrochemical deposition of Cu_2O

The electrochemical deposition of Cu_2O film was performed in a 3L glass beaker containing 0.4 M copper sulphate pentahydrate ($CuSO_4.5H_2O$, Merck, 99%) and 1.2 M citric acid ($C_6H_8O_7$, Merck, 99%) according to a procedure reported elsewhere.[17] The pH of the electrolyte was adjusted to 11 by adding sodium hydroxide (NaOH, Merck, 97%) crystals. A two-electrode setup was used in which Pt mesh was the counter electrode. A constant current value of 0.2 A was applied during the electrodeposition for varying durations. The temperature of the bath was kept at 50°C during the deposition.

2.3. Characterisation

AFM measurements were conducted with tapping mode using Hitachi 5100N equipment. XRD data were collected on a Rigaku D-Max with Cu-Kα source (1.54 Å). SEM and EDX measurements were carried out with an FEI Quanta FEG 450 scanning electron microscope. Reflectance spectra were obtained using an Ocean Optics HR4000 spectrometer at 45° incident angle. A CIE 1931 chromacity diagram was formed using the web application developed by Hasabeldaim *et al.*[18]

2.4. Adhesion test

The cross-cut tests were performed according to ISO2409 standard.[19] 10 horizontal and 10 vertical line cuts with 1 mm spacing were made using a razor blade and a template. A piece of scotch tape (3M, 2525) was attached to the grid pattern and pressed with a finger to assure a firm attachment. After waiting for 5 min, the tape was peeled off at 60° angle.

2.5. Corrosion measurements

Corrosion measurements were carried out by Gamry Interface 1000 potentiostat in a three electrode set-up where Pt wire and saturated calomel electrode (SCE) served as the counter and reference electrode, respectively. 3% NaCl solution was used as the electrolyte. The geometric area of the samples

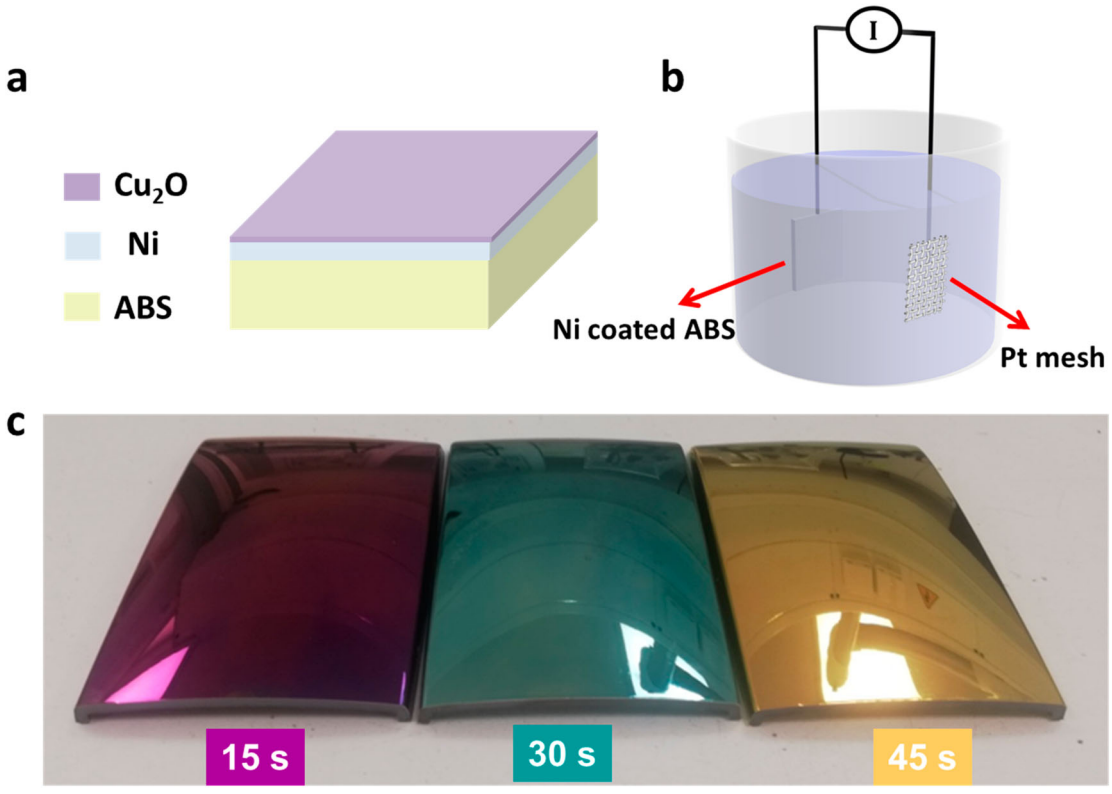

Figure 1. (a) Schematic structure of the Ni/Cu_2O bilayer film deposited on ABS substrate. (b) Two-electrode set-up used for the electrochemical deposition of the Cu_2O thin films. (c) The coloured bilayer films electrochemically deposited on large area ABS substrates.

was 2.25 cm^2. Prior to measurements, the samples were left at open circuit potential (E_{oc}) for 30 min to reach a steady state condition. Tafel plots were obtained by scanning the potential from −0.25 V to +0.25 V with respect to E_{oc} with scan rate of 0.25 mV s^{-1}. Impedance measurements were conducted between 10 and 1 MHz at E_{oc} with an excitation voltage of 10 mV.

3. Results and discussion

Figure 1a shows the schematic structure of the fabricated bilayer film on ABS substrate, which consists of a thick Ni layer and a thin Cu_2O dielectric layer. A two-electrode setup (Figure 1b) was employed for the electrodeposition of Cu_2O films on Ni-coated ABS substrates to show the industrial feasibility of the process. As the electrochemical deposition of Cu_2O can be controlled in a galvanostatic manner, a reference electrode is not necessary. Cu_2O can be deposited from alkaline Cu(II)-citrate solutions, in which citrate ions stabilise Cu^{+2}, preventing precipitation.[17,20] Depending on the current density (j), the following electrochemical reactions may take place:[17]

$$[Cu_2H_{-2}Cit_2]^{4-} + 4e^- + 2H_2O \rightarrow 2Cu + 2Cit^{3-} + 2OH^- \quad (1)$$

$$[Cu_2H_{-2}Cit_2]^{4-} + 2e^- + H_2O \rightarrow Cu_2O + 2Cit^{3-} \quad (2)$$

Here, H_{-2} denotes the detachment of β-hydroxyl group in the alkaline solution whereas Cit stands for citrate ligand. When j > 1 mA cm^{-2}, reaction (1) occurs, forming metallic Cu. Conversely, reaction (2) occurs when j < 1 mA cm^{-2}, resulting in the deposition of Cu_2O. The total surface area of the ABS substrates is 210.74 cm^2, which translates to a current density of 0.95 mA cm^{-2}. The deposition of the Cu_2O films under a current density of 0.95 mA cm^{-2} for 15, 30 and 45 s led to purple, dark cyan and gold coloured films, which implies the formation of Cu_2O (Figure 1c). The homogeneity of the colours indicates the uniform thickness of the Cu_2O films. A critical step to achieve good homogeneity was to exclude stirring of the electrolyte during the deposition. Stirring the electrolyte gave rise to

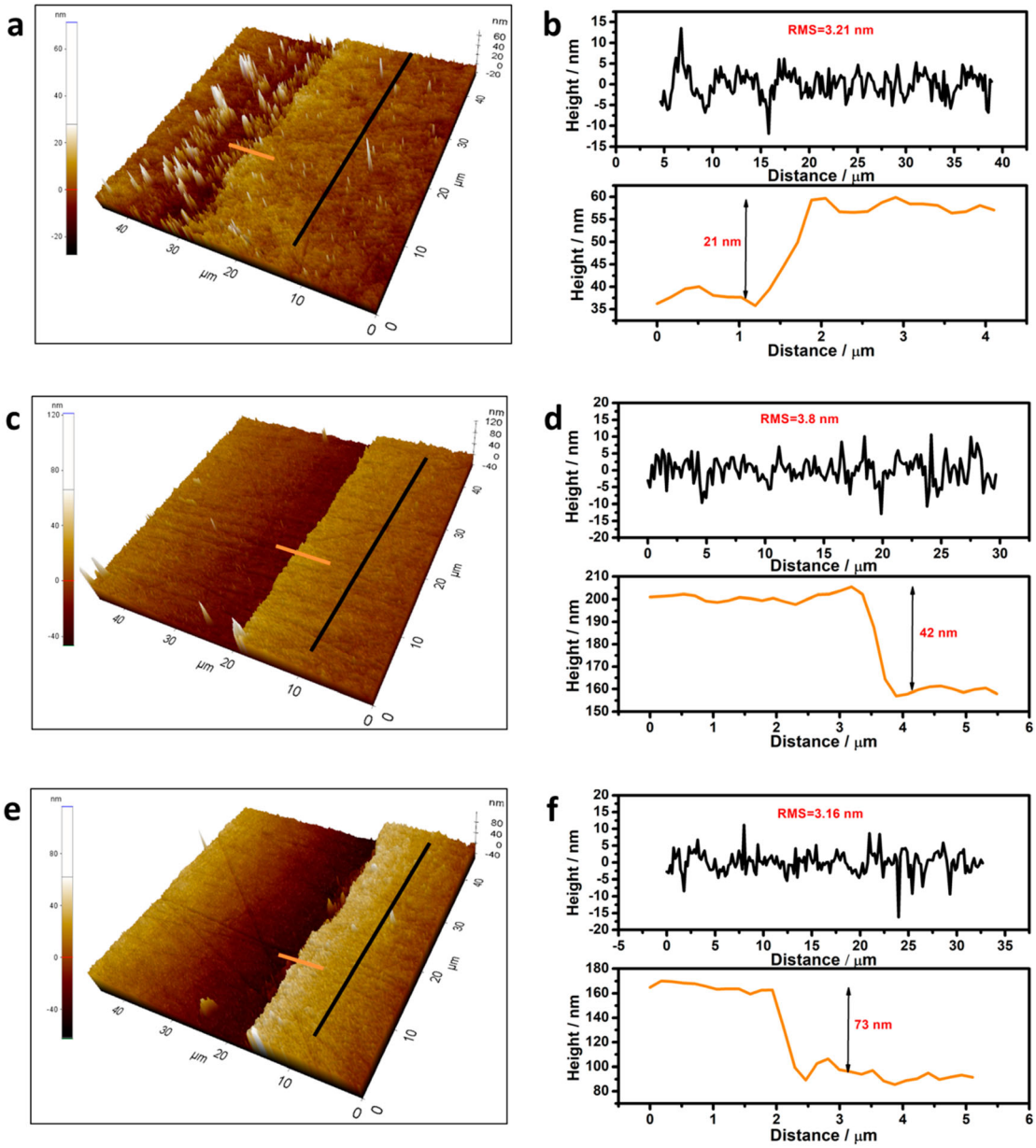

Figure 2. Topographic AFM images and the height profiles of the orange and black lines for the Cu_2O films deposited for (a) and (b) 15 s, (c) and (d) 30 s and (e) and (f) 45 s.

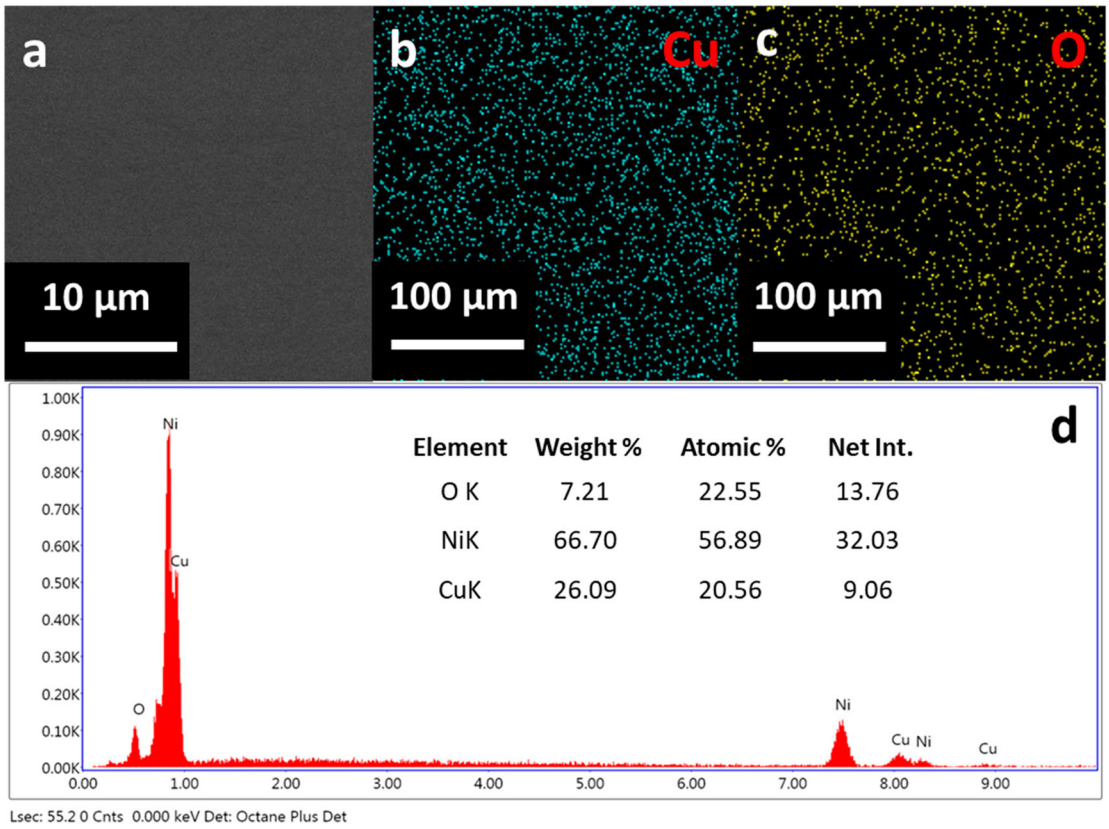

Figure 3. SEM image showing the morphology of a Cu_2O film deposited on Ni-coated ABS substrate. EDX mapping images of the (b) Cu and (c) O elements. (d) EDX spectrum of the bilayer film deposited on ABS substrate.

uneven colouration of the films due to the irregular flow of the electrolyte over the sample surface, which resulted in thickness variations. A similar observation has been made by Susetyo *et al*. who investigated the effect of stirring on the morphology of electrodeposited Ni films on Cu substrates and found that smoother films with smaller grain size could be deposited without stirring.[21] Mass transport of the ions was sufficient to support the electrochemical reactions taking place at the electrode surface as indicated by the similar deposition rates for the increasing deposition times.

AFM measurements were carried out to determine the thickness and root-mean-square (rms) roughness of the

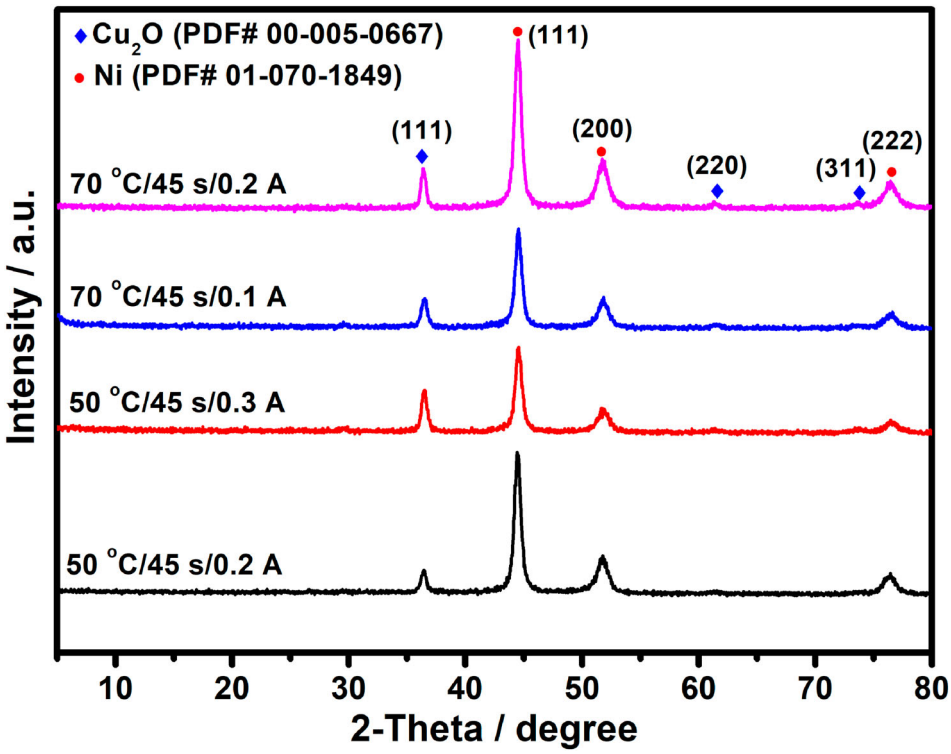

Figure 4. XRD patterns of the Ni/Cu_2O bilayer films deposited at different conditions.

Cu_2O films (Figure 2). The measured thickness values are 21, 42 and 73 nm for 15, 30 and 45 s deposition times, respectively. Nearly linear dependence of the thickness on the deposition time signifies a constant deposition rate, whose value was calculated as 1.7 nm s^{-1}. The rms roughness values calculated along the black lines on the AFM images are on the order of 3 nm. The low rms roughness values indicate a smooth surface that is essential to achieve uniform colours.

SEM image in Figure 3a clearly depicts the smooth surface of the Cu_2O film with no obvious morphological structures. The elemental mapping images of Cu and O show uniform distribution of the elements throughout the sample (Figure 3b,c). The EDX spectrum confirms that the bilayer film contains Ni, Cu and O elements (Figure 3d). No impurities such as C or Na were detected in the EDX spectrum, indicating the high purity of the Ni/Cu_2O bilayer film. Cu/O atomic ratio was found to be lower than the stoichiometric ratio of 2, most likely due to partial oxidation of the Ni surface. Moreover, similar morphologies and chemical compositions were obtained for the Cu_2O films deposited at a bath temperature of 70°C or under a current value of 0.3 A (Supplementary Figures S1 and S2).

XRD patterns of the Ni/Cu_2O bilayer films deposited under different conditions are compared in Figure 4. All samples exhibit similar diffraction patterns in which the peaks at around 36.54°, 61.29° and 73.69° correspond to the (111), (220) and (311) planes of Cu_2O (PDF# 00-005-0667) while the peaks at 44.43°, 51.77° and 76.45° match well with Ni (PDF# 01-070-1849). The sharp diffraction peaks observed for both Ni and Cu_2O indicate the high crystallinity of the bilayer film. The (111) peak of the Cu_2O has much higher intensity compared to (220) and (311), implying that the film is preferentially oriented in the (111) direction. Interestingly, deposition at 50°C under a j value of 1.4 mA cm^{-2} (0.3 A) resulted in Cu_2O rather than Cu, contrary to the observations of Eskhult and Nyholm.[17] The present authors deposited Cu_2O on Ni while Eskhult and Nyholm used a Cu substrate, which might cause different overpotentials for the electrochemical deposition of Cu_2O and, in turn, account for such discrepancy. The average grain sizes of the Cu_2O films were calculated using the Debye-Scherer equation[22], $d = [K\lambda/\beta\cos\theta]$, where d is the average grain size, K is the shape factor (0.9), λ is the X-ray wavelength (0.154 nm) and β is the FWHM. The calculation yielded a d value of 16.3 nm for the Cu_2O film deposited at 50°C under a current of 0.2 A. Such small size grains are ideal to obtain smooth films with high thickness uniformity. Increasing the current to 0.3 A or bath temperature to 70°C slightly increased the d value to 16.6 and 18.5 nm, respectively, without a significant impact on the crystal structure.

The reflectance spectra of the bilayer films acquired at 45° incident angle are displayed in Figure 5a. The samples with thin dielectric layers (21 and 42 nm) show a broad reflectance dip in the visible region. The reflection minima red shifts as the thickness of the dielectric layer increases.[23] This is in agreement with an interference effect in which the reflection minima of an optical interference coating occurs at $\lambda = 4nd$,[24] where n is the refractive index and d is the thickness of the dielectric layer. Depending on the thickness of the dielectric layer, constructive and destructive interference occurs at certain wavelengths leading to different colours. Moreover, Cu_2O is a lossy dielectric material with a complex refractive index ($N = n + ik$) whose value changes with the wavelength of the light.[24] Hence, the observed colouration effect of the Ni/Cu_2O bilayer films can be explained by the combination of the interference effect and the complex refractive index of the Cu_2O layer. Ni/Cu_2O (21 nm) bilayer film mainly reflects in blue and red region, resulting in purple colour

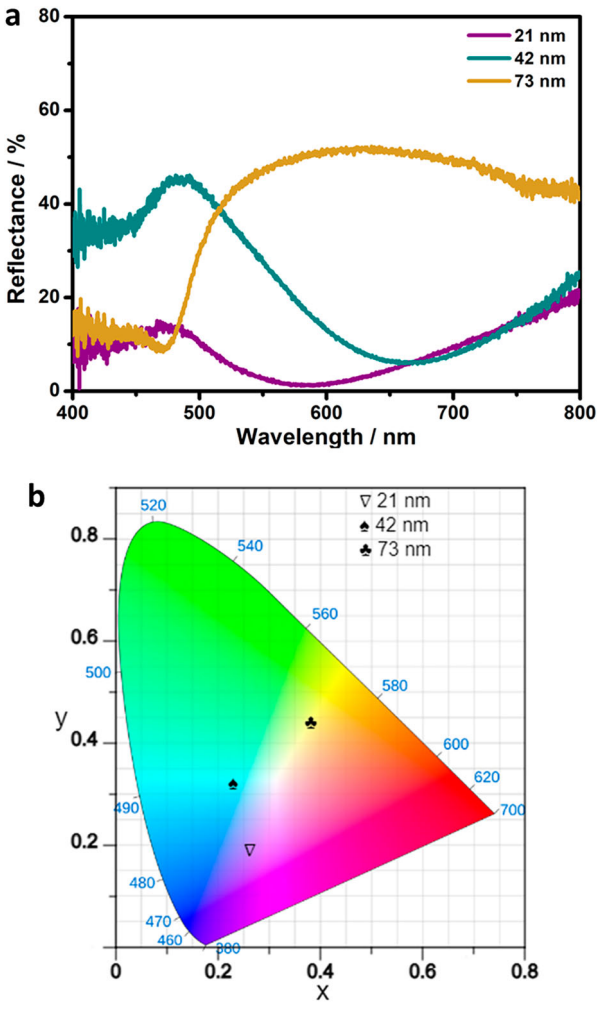

Figure 5. (a) Reflectance spectra of the Ni/Cu_2O bilayer films with varying Cu_2O thicknesses measured at 45° incident angle. (b) The colour coordinates of the samples in CIE 1931 chromacity diagram.

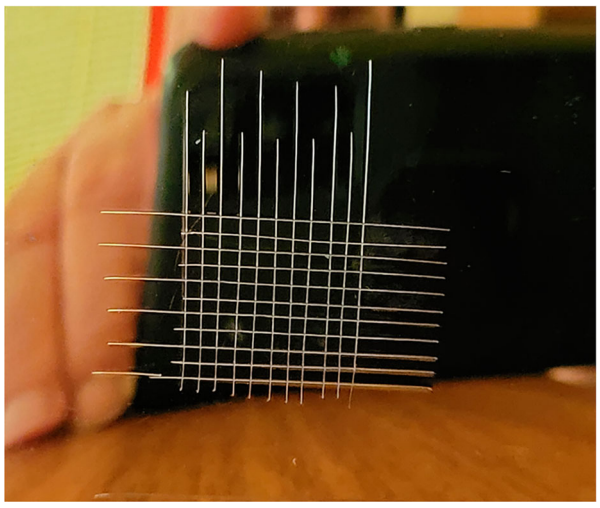

Figure 6. Cross-cut test result of the Ni/Cu_2O bilayer film coated on ABS substrate.

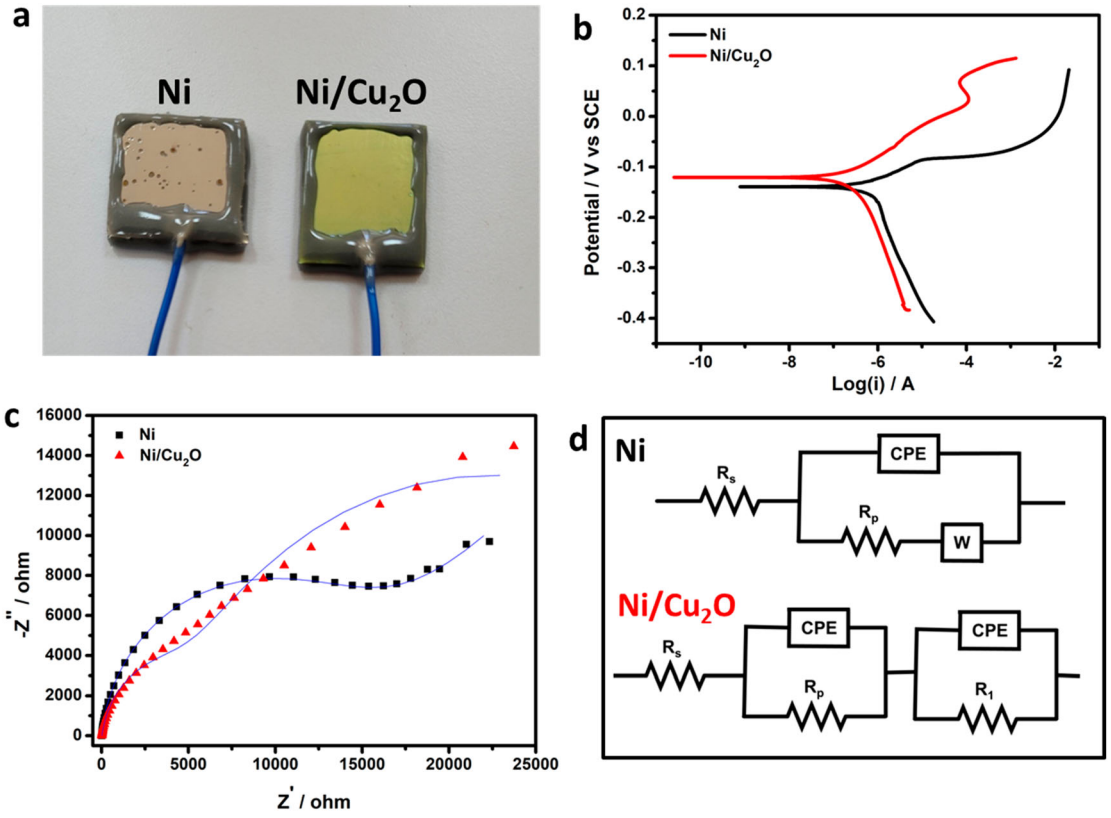

Figure 7. (a) Photographs of the Ni and Ni/Cu_2O samples after corrosion tests. (b) Tafel and (c) Nyquist plots of the samples. (d) Equivalent circuit models used to fit the impedance data.

whereas Ni/Cu_2O (42 nm) shows strong reflection of blue and yellow light, which yields a dark cyan colour. On the other hand, Ni/Cu_2O (73 nm) only reflects light between 500–800 nm, in which the combination of green, yellow and red leads to gold colour. The measured reflectance spectra are represented in a CIE 1931 chromacity diagram where the colour codes match well with the observed colours of the samples (Figure 5b).

A cross-cut adhesion test carried out in accordance with ISO 2409 standard shows the good adhesion of the Ni/Cu_2O bilayer film on the ABS substrate. Smooth cut edges with no obvious delamination in Figure 6 indicates the highest score of 0. Moreover, environmental stability of the bilayer film was tested by storing the samples for 3 months in a laboratory environment where mild solvent and acid fumes may be present. No discolouration was observed during the storage time (Supplementary Figure S3), indicating the good environmental stability of the bilayer film. Even though CuO is the thermodynamically favourable phase, it is likely that oxidation of the Cu_2O film occurs only at the surface, which does not affect the optical properties significantly. In fact, Lee *et al.* reported that the thickness of the CuO layer in ALD deposited Cu_2O films exposed to ambient air is about 1 nm.[25] The formation of the CuO layer at the surface limits the oxygen diffusion, thereby preventing further oxidation.

Table 1. The corrosion parameters extracted from the polarisation curves of the bare Ni and Ni/Cu_2O films by using the Tafel extrapolation method.

Sample	E_{corr} (mV *vs* SCE)	I_{corr} (μA cm^{-2})	β_a (mV dec^{-1})	B_c (mV dec^{-1})
Ni	−139	0.33	48	234
Ni/Cu_2O	−121	0.16	78	234

The corrosion behaviour of the Ni/Cu_2O bilayer film was studied by polarisation and impedance measurements in 3% NaCl solution. Black spots appeared on the bare Ni film after the corrosion tests indicating that the corrosion mechanism is pitting corrosion (Figure 7a). On the other hand, there is no obvious sign of corrosion on the surface of the Ni/Cu_2O bilayer film, revealing its chemical stability. The polarisation curves of the bare Ni and Ni/Cu_2O bilayer films are shown in Figure 7b. Corrosion parameters were obtained by the Tafel extrapolation of the polarisation curves (Table 1). The Ni/Cu_2O bilayer film exhibits more positive corrosion potential (E_{corr}), larger anodic Tafel slope (β_a) and lower corrosion current (I_{corr}) compared to bare Ni, clearly indicating the corrosion protective effect of the Cu_2O. Polarisation resistance (R_p) values derived by fitting Nyquist plots (Figure 7c) to suitable equivalent circuit models depicted in Figure 7d gave polarisation resistance (R_p) values of 14.79 and 37.54 kohm for the bare Ni and Ni/Cu_2O bilayer films, respectively. The larger R_p value of the Ni/Cu_2O bilayer film suggests a more passive surface and superior corrosion resistance.

4. Conclusion

In summary, the authors have demonstrated the electrochemical deposition of coloured Ni/Cu_2O bilayer films on large area ABS parts on which purple, dark cyan and gold colours could be formed by changing the deposition time. The compact structure and low roughness of the Cu_2O dielectric layer enabled even colouration across the ABS substrate. One critical factor to achieve uniform deposition of the dielectric layer was the exclusion of the electrolyte stirring which caused irregular electrolyte flow over the sample surface. Changing the deposition temperature from 50 to 70°C or

deposition current from 0.2 to 0.3 A didn't have a significant effect on the crystal structure or morphology. The Ni/Cu_2O bilayer film has a good adhesion on ABS, exhibits long-term stability in ambient air and enhanced corrosion resistance in 3% NaCl solution. The study presented here opens up the possibility of industrial scale production of coloured interference coatings for plastic substrates as an alternative to the commonly used Cr coatings.

Acknowledgements

The authors acknowledge the financial support of Durden Plastic Products and Adhesive Films Inc. Also, they would like to thank Prof. Ersin Kayahan for his help with the reflectance measurements.

Disclosure statement

In accordance with Taylor & Francis policy and my ethical obligation as a researcher, I am reporting that Alime Colak and Huseyin Balci are current employees of Durden Plastic Products and Adhesive Films Inc., which both financially supported this work and has a business interest in the research reported in the enclosed paper.

ORCID

Suleyman Can http://orcid.org/0000-0002-9297-9978
Cihan Kuru http://orcid.org/0000-0002-8565-8068

References

1. C. I. Aguirre, E. Reguera and A. Stein: *Adv. Funct. Mater.*, 2010, **20**(16), 2565–2578.
2. M. Song, D. Wang, S. Peana, S. Choudhury, P. Nyga, Z. A. Kudyshev, H. Yu, A. Boltasseva, V. M. Shalaev and A. V. Kildishev: *Appl. Phys. Rev.*, 2019, **6**(041308), 1–26.
3. Y. Kim, K. Jung, J. Cho and J. K. Hyun: *ACS Nano*, 2019, **13**(9), 10717–10726.
4. Y. Fu, C. A. Tippets, E. U. Donev and R. Lopez: *Wiley Interdiscip. Rev. Nanomed. Nanobiotechnol.*, 2016, **8**(5), 758–775.
5. T. Lee, J. Jang, H. Jeong and J. Rho: *Nano Converg.*, 2018, **5**(1), 1–21.
6. Z. Yang, Y. Chen and Y. Zhou: *Adv. Opt. Mater.*, 2017, **5**(10), 1–9.
7. H. Kocer, S. Butun, Z. Li and K. Aydin: *Sci. Rep.*, 2015, **5**(8157), 1–6.
8. C. Ji, Z. Zhang, T. Masuda, K. Yuki and L. J. Guo: *Nanoscale Horiz.*, 2019, **4**(4), 874–880.
9. Z. Li, S. Butun and K. Aydin: *Acs Photonics*, 2015, **2**(2), 183–188.
10. C. Yang, W. Shen, Y. Zhang, K. Li, X. Zhang and X. Liu: *Sci. Rep.*, 2015, **5**(9285), 1–5.
11. J. Zhao, M. Qiu and X. Yu: *Adv. Opt. Mater.*, 2019, **7**(1900646), 1–8.
12. W. Septina, S. Ikeda, M. A. Khan, T. Hirai, T. Harada, M. Matsumura and L. M. Peter: *Electrochim. Acta*, 2011, **56**(13), 4882–4888.
13. S. J. Kim, S. Kim, J. Lee, J. Yongjao, S. YuSeong, L. Myounghoon, L. Yousil, C. R. Cho, J. Kim, M. Cheon, J. Hwang, Y. I. Kim, Y. H. Kim, Y. M. Kim, A. Soon, M. Choi, W. S. Choi and Y. H. Lee: *Adv. Mater.*, 2021, **33**(2007345), 1–7.
14. Y. Su, X. Tang, G. Huana and P. Zhang: *Opt. Commun.*, 2020, **464**(125483), 1–6.
15. H. Pan, Z. Wen and Z. Tang: *Nanophotonics.*, 2020, **9**(10), 3385–3392.
16. X. Zhang, S. Jiang, M. Cai, H. Zhao, F. Pan and X. Ning: *Ceram. Int.*, 2020, **46**(9), 13342–13349.
17. J. Eskhult and L. Nyholm: *J. Electrochem. Soc.*, 2007, **155**(2), 115–122.
18. E. H. H. Hasabeldaim, H. C. Swart and R. E. Kroon: *RSC Adv.*, 2023, **13**(8), 5353–5366.
19. International Organization for Standardization (ISO). ISO 2409 paint and varnishes cross-cut test: ISO, 2013.
20. M. A. Hossain, R. Al-Gaashani, H. Hamoudi, M. Marri, I. A. Hussein, A. Belaidi and N. Tabet: *Mater. Sci. Semicond. Process.*, 2017, **63**, 203–211.
21. F. B. Susetyo, A. Faridh and B. Soegijono: *IOP Conf. Ser. Mater. Sci. Eng.*, 2019, **694**(012040), 1–6.
22. P. Debye and P. Scherrer: *Phys. Zeit.*, 1916, **17**, 277–283.
23. S. D. Wang and J. Y. Wang: *Appl. Surf. Sci.*, 2019, **476**, 1035–1048.
24. A. A. Hssi, L. Atourki, N. Labchir, M. Ouafi, K. Abouabassi, A. Elfanaoui, A. Ihlal and K. Bouabid: *Mater. Res. Express*, 2020, **7**(016424), 1–10.
25. S. W. Lee, Y. S. Lee, J. Heo, S. C. Siah, D. M. W. Chua, R. E. Brandt, S. B. Kim, J. P. Mailoa, T. Buonassisi and R. G. Gordon: *Adv. Energy Mater.*, 2014, **4**(11), 1301916.